Quasigeostrophic Turbulence in a Three-Layer Model: Effects of Vertical Structure in the Mean Shear

ISAAC M. HELD

Geophysical Fluid Dynamics Laboratory/NOAA, Princeton University, Princeton, New Jersey

ENDA O'BRIEN

Rosenstiel School of Marine and Atmospheric Science, University of Miami, Miami, Florida

(Manuscript received 28 March 1991, in final form 6 January 1992)

ABSTRACT

A three-layer, horizontally homogeneous, quasigeostrophic model is selected as one of the simplest environments in which to study the sensitivity of baroclinic eddy fluxes in the atmosphere to the vertical structure of the basic-state temperature gradients or vertical wind shears. Eddy statistics obtained from the model are interpreted in terms of linear theory and a modified "baroclinic adjustment" hypothesis. Both linear theory and the baroclinic adjustment construction are found to provide useful predictions for the vertical structure of the eddy potential vorticity flux.

For equal values of the mean vertical shear, eddy fluxes and energies are greater when the shear is concentrated at lower levels ($d^2U/dz^2 < 0$) than when the shear is concentrated at higher levels ($d^2U/dz^2 > 0$). Eddy fluxes are more sensitive to lower- than to upper-level mean temperature gradients. This relative sensitivity is a function of $\gamma = f^2\Lambda/(\beta N^2 H)$, where Λ is the mean vertical shear and H is the depth of the fluid. It is enhanced as γ is reduced, as the unstable modes become shallower, until the eddies become almost completely insensitive to the strength of the upper-layer wind for $\gamma < 0.5$.

1. Introduction

In the standard two-layer quasigeostrophic model, the relationship between the meridional potential vorticity (PV) flux F, momentum flux M, and heat flux H is

$$F_u = -\partial M_u/\partial y - \alpha H,$$

$$F_l = -\partial M_l/\partial y + \alpha H,$$

where the subscripts u and l refer to the upper and lower layers and α is a constant. If the horizontal domain is a reentrant channel bounded meridionally by rigid walls, then the horizontal average of the PV flux in the upper layer must be equal and opposite to that in the lower layer, since M vanishes at the walls.

The homogeneous turbulence studies of Salmon (1980), Haidvogel and Held (1980), and Vallis (1988), using a two-layer quasigeostrophic model with time-mean vertical shear, are in a sense fundamentally simpler than inhomogeneous turbulence studies in a channel, in that there is no time-mean momentum flux divergence. In such a model, the time-mean PV flux at any latitude in the lower layer must be equal and opposite to that in the upper layer, and knowledge of a single number (F in the lower layer, say) yields complete information about the climatological PV flux, heat flux, and eddy energy generation. (In practice, very long integrations are required to obtain nearly homogeneous statistics in such models, and one uses the average over the horizontal domain as well as over time to obtain the best estimate of the infinite-time mean at any latitude.)

As more vertical layers are included in such a homogeneous model, the vertically integrated PV flux must still be zero, but the question of how this flux is distributed in the vertical becomes an issue. Our purpose in this study is to investigate the vertical structure of the PV flux in the simplest nontrivial context, namely, that of a *three-layer* horizontally homogeneous model.

In the three-layer model, there are two "temperature gradients," corresponding to the vertical shears across the two interfaces. This is the simplest framework in which to study the effects of height-dependent shear, or the separate effects of upper- and lower-level temperature gradients, on eddy statistics. The dependence of eddy fluxes on the mean meridional temperature gradient is addressed by various eddy flux closure schemes, such as those of Stone (1972), Green (1970), and Held (1978), but the arguments underlying these

Corresponding author address: Dr. Isaac M. Held, Princeton University, Geophysical Fluid Dynamics Laboratory, P.O. Box 308, Princeton, NJ 08542.

© 1992 American Meteorological Society

"theories" are sufficiently qualitative that they give little guidance as to the dependence on temperature gradients at different levels. This issue is potentially of interest with regard to dynamics of the greenhouse warming, since general circulation models suggest that the *equilibrium* climate consistent with an increased concentration of the greenhouse gases will have smaller lower-tropospheric temperature gradients but larger upper-tropospheric gradients than does the present climate (e.g., Manabe and Wetherald 1975). [But see also Stouffer et al. (1989) in which temperature gradients increase at all levels during the *transient* response in the Southern Hemisphere.]

2. The model

The model used in this study is a three-layer version of that used by Haidvogel and Held (1980, hereafter referred to as HH), with a modified (more scale-selective) subgrid-scale mixing formulation. There are other examples of homogeneous quasigeostrophic turbulence calculations in multilayer models, including some with imposed mean vertical shear [e.g., the four vertical-mode model of Hua and Haidvogel (1986)]; but these have typically focused on problems related to spectral shape and Charney's (1971) analogy between quasigeostrophic and two-dimensional turbulence, rather than on the issues outlined herein.

Our starting point is a Boussinesq fluid with constant stratification N^2 on an infinite β plane. The equation of motion and boundary conditions are

$$\partial_t Q + J(\Psi, Q) = -\nu\nabla^8 Q, \quad 0 < z < H, \tag{1a}$$

$$\partial_t \Psi_z + J(\Psi, \Psi_z) = -\nu\nabla^8 \Psi_z, \quad z = H, \tag{1b}$$

$$\partial_t \Psi_z + J(\Psi, \Psi_z) = -\nu\nabla^8 \Psi_z - \kappa H\epsilon^{-1}\nabla^2\Psi, \quad z = 0, \tag{1c}$$

where J is the horizontal Jacobian operator, $\nabla^8 \equiv (\nabla^2)^4$ where ∇^2 is the horizontal Laplacian, ν is the constant hyperdiffusivity, $\epsilon \equiv (f/N)^2$, κ is the reciprocal of the e-folding time for a barotropic eddy due to Ekman pumping at the ground, and

$$Q = \nabla^2\Psi + \beta y + \epsilon\Psi_{zz}. \tag{2}$$

Here Ψ is the total streamfunction, which is decomposed into a constant background flow (which provides the energy source for the system) and a dynamically active part:

$$\Psi(x, y, z, t) = -U(z)y + \psi(x, y, z, t). \tag{3}$$

To avoid a common misconception about such models, we emphasize that ψ has zonally symmetric as well as zonally asymmetric components. The Ekman pumping is confined to the lower boundary to mimic the situation in the atmosphere.

The equations are nondimensionalized using the velocity, horizontal length, vertical length, and time scales (ΛH, NH/f, H, $N/(f\Lambda)$), where Λ is the mean vertical shear, $(U(H) - U(0))/H$. The nondimensional parameters in the problem become

$$\kappa_* \equiv \kappa N/(f\Lambda),$$

$$\nu_* \equiv (NH/f)^8(N/f\Lambda)\nu,$$

$$\gamma \equiv f^2\Lambda/(\beta N^2 H). \tag{4}$$

We use the same notation for dimensional and nondimensional variables as long as there is no likelihood of confusion; where the distinction is necessary, the dimensionless variable is marked by an asterisk.

Dividing the flow into M layers in the usual way (Pedlosky 1987), with $i = 1$ at the bottom and $i = M$ at the top, the governing nondimensional equations become

$$\partial_t q_i + \psi_{i,x}Q_{i,y} + U_i q_{i,x} + J(\psi_i, q_i) = -\nu\nabla^8 q_i - \delta_{i1}\kappa M\nabla^2\psi_i, \quad i = 1, M, \tag{5}$$

where δ_{ij} is the Kronecker delta, while

$$q_i = \nabla^2\psi_i + M^2(\psi_{i+1} - 2\psi_i + \psi_{i-1}), \tag{6a}$$

and

$$Q_{i,y} = \gamma^{-1} - M^2(U_{i+1} - 2U_i + U_{i-1}). \tag{6b}$$

To satisfy the boundary conditions in this discrete framework, one need only set $\psi_0 = \psi_1$ and $\psi_{M+1} = \psi_M$ in (6a) and $U_0 = U_1$ and $U_{M+1} = U_M$ in (6b). Calculations with large M are currently in progress; here we restrict attention to the case $M = 3$.

In this three-layer case, we set $U_1 = 0$ and $U_3 = 1$, so the vertical structure of the mean flow is completely specified by the value of

$$U_2 \equiv (1 - \alpha)/2, \tag{7}$$

where α is proportional to the curvature of the flow:

$$\partial^2 U/\partial z^2 \approx (1 - 2U_2)/(\Delta z)^2 = 9\alpha. \tag{8}$$

If $\alpha = 1$ ($\alpha = -1$), the vertical shear is entirely confined to the upper (lower) two layers. If $\alpha = 0$, the two vertical shears in the model are equal.

3. Linear modes

Before presenting the results for the full model, it is instructive to consider some properties of the linear modes. [Davey (1977) discusses the linear inviscid three-layer model in some detail.] Discarding the nonlinear term in (5), we seek solutions of the form

$$\psi_i = \mathrm{Re}\{A_i e^{i(kx+ly-\sigma t)}\}. \tag{9}$$

In the three-layer model, there are three complex roots σ for each (k, l) pair. The most unstable mode always occurs for $l = 0$.

Fixing $\kappa = 0.1$, $\nu = 3 \times 10^{-7}$ (values that will be used in our nonlinear calculations), and $\alpha = 0$, Fig.

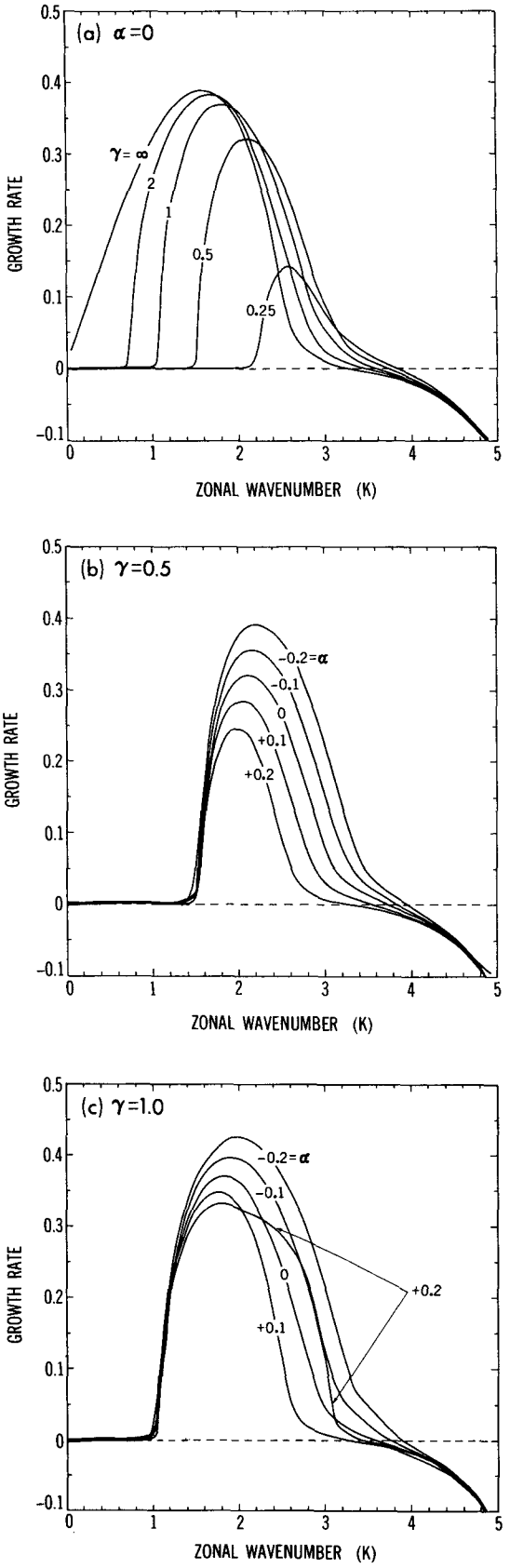

1a shows the nondimensional growth rate of the most unstable mode as a function of k (with $l = 0$) for five different values of γ. Figures 1b and 1c are similar plots for five different values of the curvature α, with $\gamma = 0.5$ and $\gamma = 1.0$, respectively. (The damping at large wavenumbers is caused by the hyperdiffusivity.) As γ increases, the maximum growth rate (ω_m) increases and the wavenumber of maximum instability (k_m) decreases. Once γ increases beyond ≈ 2, ω_m and k_m have more or less asymptoted to their $\gamma \to \infty$ ($\beta \to 0$) limit, although small wavenumbers continue to be destabilized.

The maximum growth rate ω_m also increases as α becomes more negative, corresponding to vertical shear that is concentrated at low levels, while k_m increases by a modest amount. Inspection of the vertical structure of the most unstable mode shows that the streamfunction amplitude and westward phase tilt are both enhanced at low levels when the vertical shear is concentrated there, consistent with multilayer results described, for example, in Satyamurty et al. (1982) and Staley (1986). Comparing Figs. 1b and 1c, one sees that the effect of the curvature α on the growth rate is weakened when γ increases. Note also that the curve for $\gamma = 1$ and $\alpha = +0.2$ in Fig. 1c has a somewhat different character than the others, a point that we return to later.

The curves in Fig. 1 all show very small but positive growth rates at small wavenumbers. These waves are slightly destabilized by the surface friction. As described by Davey (1977), there is a long-wave cutoff in the inviscid three-layer model, just as in the more familiar two-layer case. Unstable Green modes make their appearance only as the number of levels is increased further.

The mean PV gradients in the three layers are

$$\partial Q_1/\partial y = \gamma^{-1} - 9(U_2 - U_1) = \gamma^{-1} - 9(1 - \alpha)/2,$$
$$\partial Q_2/\partial y = \gamma^{-1} - 9(U_3 - 2U_2 + U_1) = \gamma^{-1} - 9\alpha,$$
$$\partial Q_3/\partial y = \gamma^{-1} + 9(U_3 - U_2) = \gamma^{-1} + 9(1 + \alpha)/2. \quad (10)$$

In the absence of the damping terms, baroclinic instability requires that this gradient takes on both positive and negative signs. Figure 2 shows the signs of $\partial Q_1/\partial y$ and $\partial Q_2/\partial y$ in $\alpha - \gamma$ (curvature − mean vertical shear) space. Restricting consideration to positive γ and $\alpha > -1$, the gradient in the top layer, layer 3, is always positive. We will further restrict our study to values of α less than $1/3$, so as to avoid the region in which the

FIG. 1. Linear growth rates for the three-layer model as a function of zonal wavenumber (setting the meridional wavenumber equal to zero), with surface friction $\kappa = 0.1$ and biharmonic diffusion $\nu = 3 \times 10^{-7}$: (a) for values of the shear parameter γ ranging from 0.25 to ∞, with zero curvature $\alpha = 0$; (b) for values of the curvature α from −0.2 to 0.2, with $\gamma = 0.5$; (c) as in (b), but with $\gamma = 1.0$.

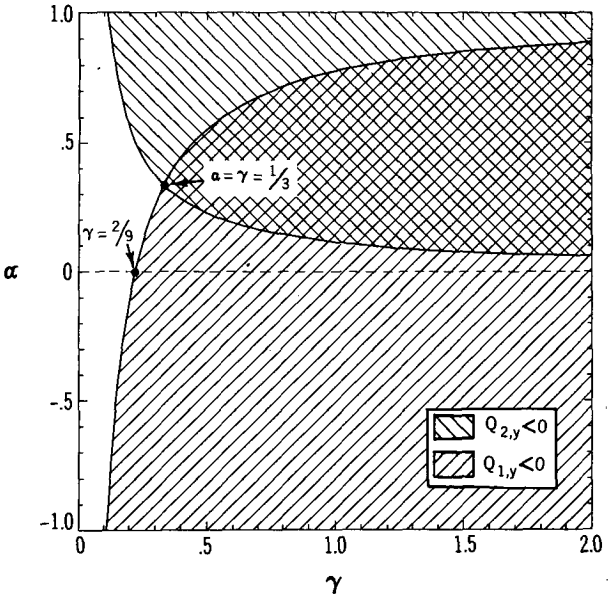

FIG. 2. The sign of the mean potential vorticity gradients in curvature (α) – vertical shear (γ) space. In this part of the parameter space, the gradient in layer 3 is always positive.

PV gradient is negative in the middle layer and positive in the lower layer, a configuration with little relevance to the atmospheric general circulation. In this restricted region of parameter space, if $\gamma < 2/[9(1-\alpha)]$ the inviscid flow is stable, if $2/[9(1-\alpha)] < \gamma < 1/(9\alpha)$ the flow is unstable, with only the lower-layer gradient being negative, and if $\gamma > 1/(9\alpha)$ the flow is unstable with the gradient being negative in the lowest two layers.

Of the curves in Fig. 1, the case $\gamma = 1$ and $\alpha = +0.2$ lies in the region where the gradient is negative in the lowest two layers. This helps explain the distinctive character of the growth-rate spectrum for this case. In all of the other cases, the negative gradient is confined to the lowest layer only. We concentrate our attention on this latter, more familiar, configuration.

Negative values of α increase the vertical shear between the lowest two levels, between which there is a sign reversal in the mean PV gradient. Positive α increases the shear between the upper two layers, which [if $\alpha < 1/(9\gamma)$] have the same sign of PV gradient. Since the sign reversal is essential to the instability, this provides an intuitive explanation for the increase in growth rate with decreasing α shown in Fig. 1.

The momentum flux convergence in modes of the form (9) is identically zero, so the sum of the PV fluxes in the three layers must vanish identically. The vertical structure of the PV flux in an unstable mode can, therefore, be described by one number,

$$r = -\overline{v_3' q_3'}/\overline{v_1' q_1'}, \tag{11}$$

the ratio of the (negative of the) top-layer eddy PV flux to that in the bottom layer. Figure 3a shows r for the most unstable mode over the range of α and γ for which we shall be performing the nonlinear calculations (fixing $\kappa = 0.1$).

In an unstable mode, the PV flux is always directed down the mean PV gradient. If $\alpha = \gamma^{-1}/9$, the PV gradient and the PV flux in the middle layer both vanish, and $r = 1$. As γ decreases, with fixed α, some of the bottom-layer flux is compensated in the middle rather than top layer, so that $r < 1$, and the mode is more confined to the lower layers. Increasing α counterbalances this effect; it increases the PV gradient in the top and bottom layers at the expense of the gradient in the middle layer, creating a deeper mode and a larger value of r.

4. Baroclinic adjustment

An alternative way of estimating how γ and α affect the vertical penetration of the eddies is through a variant of the "baroclinic adjustment" hypothesis, as discussed for a continuous atmosphere by Lindzen and Farrell (1980). The three-layer version of this argument proceeds as follows.

Consider the flow in which initially the PV gradients are given by (10). Suppose an eddy grows until it adjusts the negative gradient in the lowest layer back to zero *in part of the domain* by reducing the vertical shear between the lowest two layers, $U_2 - U_1$, to the value $(9\gamma)^{-1}$. (This homogenization can only be a local and temporary one in our model; the eddies cannot modify the spatially averaged PV gradient or vertical wind shear, and, if the statistics are spatially homogeneous, they cannot change the time-mean shear at any location.) This adjustment will also *decrease* the PV gradient in the middle layer by increasing the vertical curvature of the wind, so that now

$$\partial Q_2/\partial y|_{\text{new}} = \partial Q_2/\partial y - |\partial Q_1/\partial y| = 2\gamma^{-1} - 9(U_3 - U_2).$$

If the middle-layer gradient is positive after this modification, then it is assumed that the eddy will be confined to the lowest two layers only; it has no need to extend farther upward to stabilize the flow. This will occur if $\gamma < 2[9(U_3 - U_2)]^{-1} = 4[9(1+\alpha)]^{-1}$. In this case, one expects $r = 0$, that is, no PV flux in the top layer.

If instead the middle-layer gradient is now negative, the vertical shear between the upper two layers will have to be modified so as to bring this gradient back to zero. For the purposes of this construction, one can think of the eddy development as a two-stage process: First there are equal and opposite PV fluxes in the bottom two layers during the stage in which the lower-layer gradient is set to zero; then there are equal and opposite fluxes in the top two layers to reset the middle-layer gradient to zero. If we denote the ratio of the fluxes in the second stage to those in the first stage by ξ, the total fluxes in layers 1, 2, and 3 will be in the

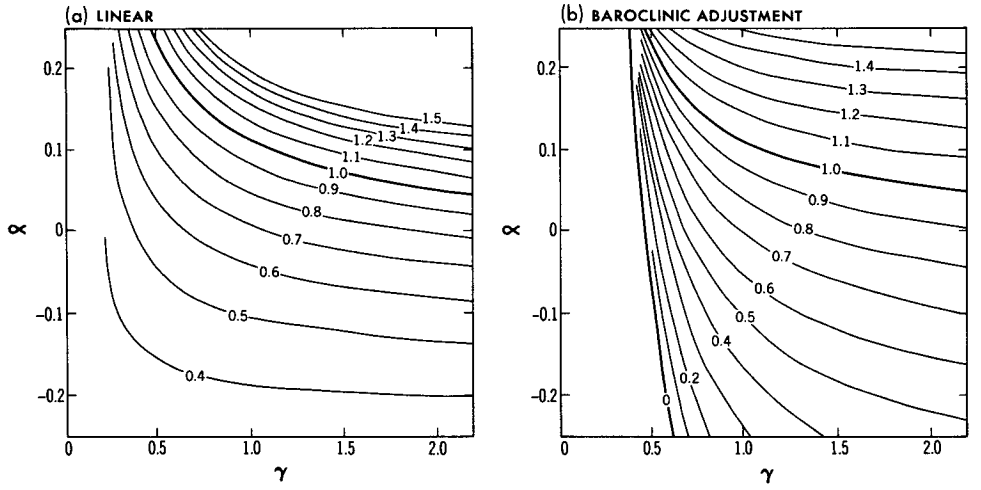

FIG. 3. (a) The ratio r, defined by (11), for the most unstable linear mode, as a function of α and γ, with $\kappa = 0.1$. (b) The ratio r predicted by the baroclinic adjustment construction.

ratio $1: \xi - 1: -\xi$, so that $r = \xi$. We are assuming here that the eddy fluxes have the same meridional scale in each layer, so that the required fluxes are proportional to the change in the PV gradient. One finds in this way that

$$r = \frac{9(U_3 - U_2) - 2\gamma^{-1}}{9(U_2 - U_1) - \gamma^{-1}} = \frac{9\gamma(1+\alpha) - 4}{9\gamma(1-\alpha) - 2}$$
$$= \frac{|\partial Q_1/\partial y| - \partial Q_2/\partial y}{|\partial Q_1/\partial y|}. \quad (12)$$

Note that this expression satisfies the requirement that $r = 1$ when $\gamma^{-1} = 9\alpha$, that is, when the initial middle-layer PV gradient vanishes.

This prediction for r as a function of γ and α is shown in Fig. 3b for comparison with that obtained from the most unstable linear mode. The $r = 1$ curves are identical in the two panels. When $\alpha = 0$, the linear mode predicts deeper PV flux than the baroclinic adjustment at small values of γ, and a shallower flux when γ is large. The difference between the two predictions is largest when γ is small and α negative.

5. The turbulence model and its horizontal spectra

Horizontally homogeneous turbulence is generated by assuming that ψ_i is doubly periodic in a square domain of width $2\pi L$. Expanding in a Fourier series,

$$\psi_i(x, y, t) = \sum_{k=-m}^{m-1} \sum_{l=-m}^{m-1} \psi_i(k, l, t) e^{i(kx+ly)\Delta}. \quad (13)$$

Here m is the number of wavenumbers retained and $\Delta = L^{-1}$ is the nondimensional grid spacing in wavenumber space, which is taken to be equal in the k and l directions. The reality of ψ requires that $\psi(k, l) = \psi^*(-k, -l)$. For the following three-layer calculations, we set $m = 32$ and $\Delta = 0.15$. While geostrophic turbulence calculations have been performed at much higher resolution, we require a large number of well-defined statistically steady states, forcing us to use a model with a modest spectral range. The resulting system is integrated in time using a leapfrog differencing scheme with a Robert filter to damp the computational mode. The nonlinear terms are computed without aliasing error using the transform method. The nondimensional time step ranges from 0.005 for the most energetic experiments, to 0.025 for the least energetic cases.

More than 50 statistically steady states have been obtained for this model for a variety of settings of the nondimensional parameters. We briefly describe the horizontal spectra in one of these states and then, in the following sections, focus on the dependence of horizontally averaged statistics on the model parameters.

The time-mean total energy budget of the model may be expressed as

$$\partial E(k, l)/\partial t = 0$$
$$= G(k, l) + S(k, l) + D(k, l) + T(k, l). \quad (14)$$

Here E, G, S, D, and T represent, respectively, the energy (available potential plus kinetic), energy generation, dissipation due to surface friction, dissipation due to diffusion, and the nonlinear transfer of energy from one wavenumber to another. Expressions for E, G, S, and D follow easily from the equation of motion. The energy transfer spectrum $T(k, l)$ is most easily computed as a residual in (14).

The time-averaged spectra of G and T are shown in Fig. 4 for $\gamma = 0.5$, $\kappa = 0.1$, and $\alpha = 0$. The spectra are normalized as in *HH*. Also shown for comparison is the linear growth rate as a function of k and l for these same parameters. These spectra are similar in structure to those of the two-layer model of *HH*. The generation

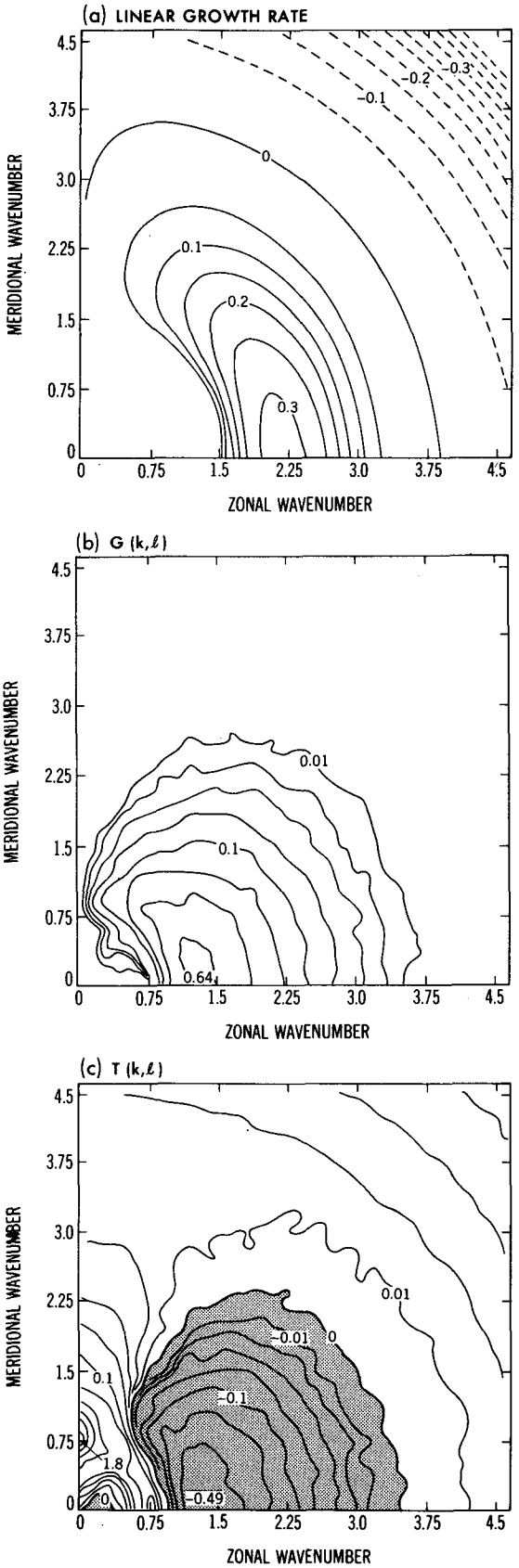

spectrum (Fig. 4b) has a similar shape to that of the growth rate spectrum, but shifted to substantially smaller wavenumbers. The maximum in G is at $(k, l) = (1.3, 0)$ while the maximum linear growth rate occurs at $(k, l) = (2.2, 0)$. This displacement of the generation toward smaller values of k becomes more pronounced as γ increases, while increasing the damping, κ, reduces the displacement. It is not surprising to find the energy move to large scales in quasi-two-dimensional turbulence, but it is of interest that the energy *generation* can itself be displaced to large scales with very small linear growth rates on the time-mean flow. The same phenomenon occurs in two-layer calculations.

Energy is transferred by nonlinear interactions from the shaded to the unshaded region in Fig. 4c, with maximum transfer out of those wavenumbers near the maximum in G. The longest zonal scales are the principal beneficiaries of the energy transfer. In fact, much of transfer is focused into wavenumber (0.0, 0.75), which corresponds to a zonal flow with alternating easterly and westerly jets repeating five times in the meridional direction (the fundamental wave has $l = 0.15$). This jet-formation phenomenon is characteristic of geostrophic turbulence on a β plane (Rhines 1975). The zonal jets that are generated have similar properties to those in the two-layer model as well as the wave–mean-flow interaction model of Panetta and Held (1988). They can be very persistent and organize the eddy activity into well-defined storm tracks. Why these inhomogeneities should have such long persistence in a model with homogeneous forcing remains an unsolved problem.

6. Vertical structure of the PV flux

From the statistics of the nonlinear model, we have computed the ratio r, defined by Eq. (11), as a function of the nondimensional parameters: γ, κ, and α. We can compare the nonlinear result with the prediction based on the most unstable linear modal structure on the one hand, and the "baroclinic adjustment" construction on the other. Recall that when $r = 0$ the bottom-layer flux is balanced by a flux in the middle layer, and the upper-layer flux is zero; when $r = 1$, the middle-layer flux is zero and the lower-layer flux is balanced by a flux in the upper layer; when $r > 1$, the flux in the middle layer is of the same sign as that in the lower layer, and the upper-layer flux balances their sum.

In both the full model and the linear mode structures,

FIG. 4. (a) Growth rate of linear modes, for $\gamma = 0.5$, $\alpha = 0$, $\kappa = 0.1$, and $\nu = 3 \times 10^{-7}$, as function of zonal (k) and meridional (l) wavenumber. (b) Energy generation spectrum, $G(k, l)$. (c) Energy transfer spectrum, $T(k, l)$. The contour intervals in (b) and (c) are logarithmic, the contour values being $10^{n/4}$ for integer n. The G spectrum is normalized so that the integral over $(0 \leq k \leq +\infty, -\infty \leq l \leq +\infty)$, using the symmetry $G(k, l) = G(k, -l)$, is equal to the energy generation, averaged in the vertical, per unit horizontal area; T is normalized consistently.

r is almost independent of the surface friction κ, for $\kappa < 0.3$. (The baroclinic adjustment construction makes no reference to κ.) This is true despite the fact that the *amplitude* of the eddies in the nonlinear model is very sensitive to κ, as emphasized in section 7. As κ varies from 0.05 to 0.3, with $\gamma = 1.0$ and $\alpha = 0$, r varies by only 13% in the nonlinear model, while the energy level in the flow varies by nearly a factor of 30.

Figure 5a compares the variation of r in the nonlinear model as a function of γ, holding $\kappa = 0.1$, $\alpha = 0$, and $\nu = 3 \times 10^{-7}$, with the value for the linear most unstable mode and the prediction of the baroclinic adjustment construction. The linear modal structure is a better predictor of the vertical structure of the nonlinear model's PV flux than is the baroclinic adjustment when $\gamma < 0.5$. In this region the latter predicts that only the lowest two layers will be dynamically active, whereas, in fact, the linear modes extend somewhat into the top layer, so one does not expect the nonlinear model's PV flux to vanish identically in that layer. The linear most unstable mode underestimates the vertical extent at large γ, but overestimates it at small γ. The baroclinic adjustment works very well at large γ.

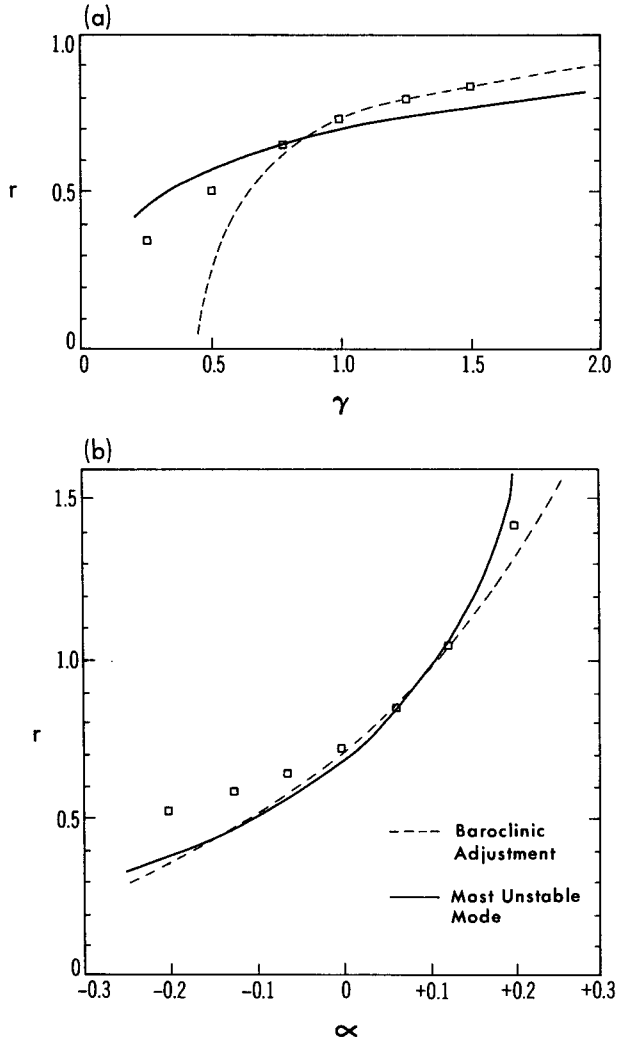

FIG. 5. (a) The values of r predicted by the nonlinear turbulence model as a function of γ with $\alpha = 0$, $\kappa = 0.1$, and $\nu = 3 \times 10^{-7}$ (small squares), the values for the most unstable linear mode (solid line), and those predicted by the baroclinic adjustment construction (dashed line). (b) Same as (a) but as a function of α, with $\gamma = 1.0$.

The close agreement between the linear most unstable mode and the nonlinear model is striking, since the maximum eddy energy generation occurs at larger horizontal scales than does the maximum linear growth rate. (Similar agreement has recently been obtained with a ten-layer model.) The difference between the generation scale and the scale of the most unstable wave increases as the flow rapidly becomes more energetic with increasing γ and decreasing κ. For example, maximum energy generation occurs at $k = 0.6$ when $\gamma = 1.0$ and $\kappa = 0.1$, while the linearly most unstable mode occurs at $k = 1.9$. The linear modes have the property that longer waves are more deeply penetrating and have larger values of r. [For the linear modes, the value of r typically increases by a modest amount as the wavenumber is reduced below that for the most unstable mode, and then decreases abruptly as the growth rates plunge to very small values (see Fig. 1).] As the generation shifts to longer waves with increasing γ, one might anticipate that linear theory at the most unstable wavenumber would underestimate r, as in Fig. 5a. However, if one tries to predict r by using the linear structure at the wavenumber of maximum energy generation, the comparison with the nonlinear model is very poor. In many cases, there is effectively no modal instability on the imposed mean flow at the wavenumber of maximum energy generation.

By any measure, the model is strongly nonlinear. As one can see from Fig. 4 for $\gamma = 0.5$, in the region of maximum energy generation it is the nonlinear transfer that is primarily balancing the generation, and not dissipation. Why the linear most unstable mode should predict the vertical structure of the PV flux this well is unclear. The "environment" that a typical eddy actually feels is very different from the imposed time-mean flow, particularly because of the existence of the persistent jets. Perhaps the structure of the PV flux is optimal in some appropriate sense for both the turbulence model and the most unstable modes in the linear model.

Figure 5b is a similar plot, but as a function of α, with $\gamma = 1.0$. All three curves must pass through the value $r = 1$ when $\alpha = 1/9$. Once again, linear theory provides a good approximation to the nonlinear model's vertical structure, although the error grows to $\sim$25% at the smaller values of α shown. The baroclinic adjustment also performs well. This agreement suggests that the physical picture underlying this construction has some value.

The values of r generated by the nonlinear model throughout the γ–α plane are displayed in Fig. 6. The

contours are drawn subjectively. This result is to be compared with the predictions in Fig. 3. The largest discrepancy with the linear modal structure occurs for small γ and negative α, where the nonlinear model's r values are less sensitive to α.

7. Magnitude of the eddy flux

We now describe how the magnitude of eddy fluxes varies as a function of three important nondimensional parameters: the mean vertical shear γ, surface friction κ, and curvature α, with emphasis on the latter. We focus on the potential vorticity flux in the lowest layer F_1. Note that $F_2 = (r-1)F_1$ and $F_3 = -rF_1$, where r is the ratio discussed in the previous section. Also, the heat or buoyancy fluxes at the upper and lower interfaces are proportional to $-F_3$ and F_1, respectively, while the eddy energy generation G is proportional to the vertical integral of the PV flux weighted by $(-U)$. (Since $U_1 = 0$, G is proportional to $-F_3 - [(1-\alpha)/2]F_2 = \{r + [(1-\alpha)/2](1-r)\}F_1$.) Thus, the two quantities F_1 and r carry most of the information of interest concerning the domain-averaged eddy statistics.

The relation between the dimensional and nondimensional PV flux is

$$F = \overline{v'q'} = \Lambda^2 H(f/N) F_*(\gamma, \kappa, \alpha). \qquad (15)$$

The factor in front of the nondimensional function F_* can be understood by thinking of $v' \approx H\Lambda$ and $q' \approx (H\Lambda)/(NH/f)$. If one ignores variations in F_*, then this scaling of the eddy flux is essentially equivalent to the scheme of Stone (1972).

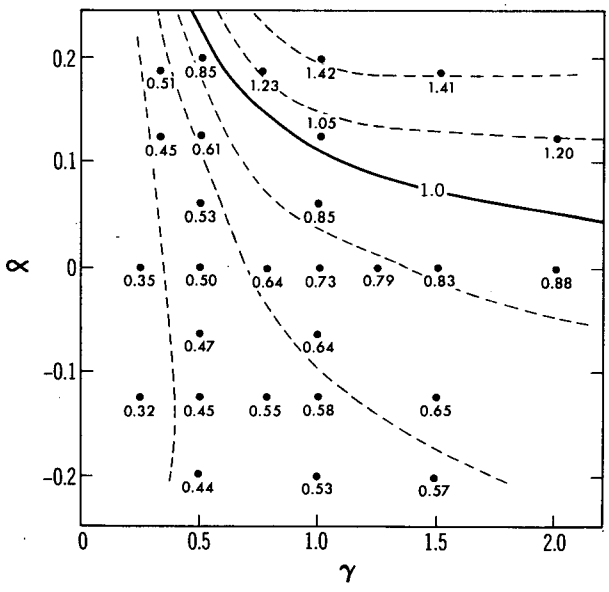

FIG. 6. The values of r obtained from the nonlinear model in the α–γ plane. Contours are drawn subjectively.

We have certain expectations concerning the dependence of F_* on α. When α decreases, the vertical shear between the lowest two layers increases, while that between the upper two levels decreases. As discussed in the context of the linear-mode growth rates, since the potential vorticity gradient changes sign between the lowest two levels, one anticipates a larger eddy energy level and larger eddy fluxes for smaller α. The fact that the linear growth rate increases with decreasing α reinforces this expectation. However, there is a competing effect: as α decreases, the eddy fluxes do not penetrate as deeply (Fig. 6), and, as argued in Held (1978), this will have the effect of reducing eddy amplitudes. The argument is that shallower eddies will also have smaller meridional particle displacements in a turbulent quasigeostrophic flow, and will be able to tap less of the mean available potential energy. The relative importance of these two effects is difficult to anticipate.

Figure 7 shows how the nonlinear model's F_1 varies with the parameters γ, κ, and α. Three cross sections of this three-dimensional parameter space are shown: the $(\gamma$–$\alpha)$ plane with $\kappa = 0.1$; the $(\kappa$–$\alpha)$ plane with $\gamma = 1.0$; and the $(\gamma$–$\kappa)$ plane with $\alpha = 0$. The contours are subjectively drawn.

These results show that the sensitivity to the curvature α is qualitatively similar at nearly all the values of γ and κ examined. *The flux increases with decreasing* α. We can conclude that *for a fixed vertically averaged vertical shear, the flux in this model is increased by concentrating the shear in the lower part of the domain.* The implication is that the effects of the changing vertical scale of the eddies is of less importance than the vertical shear in the region of reversed PV gradient. The only exception is the slight increase in F_1 as α is increased from 0.125 to 0.2, with $\gamma = 1.0$ and $\kappa = 0.1$, which is evidently related to the fact the $\alpha = 0.2$ case lies in the region with negative PV gradient in the middle layer.

A striking aspect of these results is the very strong sensitivity of the flux to γ, even when the value of γ is sufficiently large that the growth rate of the most unstable mode has asymptoted to its $\gamma \to \infty$ limit. (Compare the maximum growth rates for $\gamma = 1$ and $\gamma = 2$ in Fig. 1, and note that the PV fluxes in these two cases differ by a factor of 5.) Growth rates on the long-wave side of the most unstable wave continue to increase as γ increases, raising the possibility that these long-wave growth rates may play an important role in determining the equilibrium energy level in the flow. An alternative explanation for this sensitivity is suggested by the observation that as γ increases, energy no longer accumulates in zonal jets, since the effective strength of the β effect is weakened. The jets could be playing an important role in stabilizing the eddies, perhaps in the way argued by James (1987).

The PV flux increases with decreasing κ, except possibly at very small values of γ. This dependence is especially strong at large γ. A theory for this sensitivity

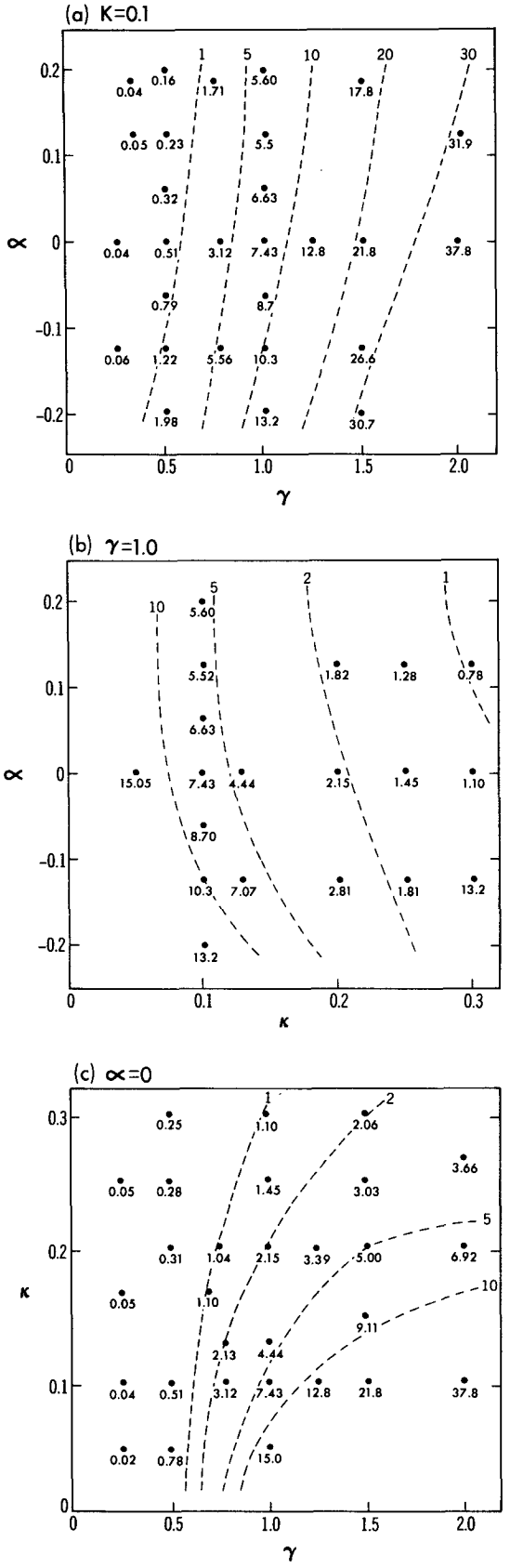

is essential to any attempt at explaining the fluxes produced by this model.

8. Sensitivity to changes in upper- and lower-level vertical shear

A change in the dimensional vertical shear between the upper or lower two layers changes all three nondimensional parameters, γ, α, and κ. For example, if the low-level shear $S_1 \equiv U_2 - U_1$ is increased, holding the upper-level shear $S_2 = U_3 - U_2$ fixed, then α decreases, but γ increases and κ decreases, since these are nondimensionalized by the vertically integrated shear $S_1 + S_2 = U_3 - U_1$. If the upper-level shear increases, holding S_1 fixed, then γ increases and κ decreases as before, while α increases. From the dependence of the potential vorticity flux on α described in section 7, it is clear that the flux is more sensitive to lower- than to upper-tropospheric shears, but it is not immediately clear from these results *how* much more sensitive.

We increase the *dimensional* vertical shear in the upper level by 10%, holding all other dimensional parameters fixed, and compute the percentage by which the dimensional flux increases. The calculation is then repeated for a 10% decrease in the shear. We average these two numbers together to estimate the sensitivity of the flux to a small change in shear. The same calculation is repeated, changing instead the lower-layer shear. These quantities are obtained using an unperturbed state with $\alpha = 0$ and $\kappa = 0.1$, and several different values of γ. The results are plotted in Fig. 8 as a function of γ. Also included in the plot is the ratio (sensitivity to lower-level shear)/(sensitivity to upper-level shear).

The large sensitivities obtained, as large as 70% for a 10% increase in the low-level shear when $\gamma = 2.0$, are themselves of interest, as they indicate how strongly baroclinic eddies resist changes in the meridional temperature gradient. They can be understood as due, first of all, to the fact that the dimensional flux (15) is proportional to the square of the shear, and, in addition, that the nondimensional flux increases quite rapidly with the increase in γ and decrease in κ that correspond to an increase in shear.

Based on the baroclinic adjustment argument and/or linear-mode structures, we expect upper-level shears to become less relevant as γ decreases, since the eddies are becoming shallower. We clearly see this tendency in Fig. 8. The sensitivity to the low-level shear is a factor of 2 greater than the sensitivity to the upper-level shear for $\gamma = 1$, and a factor of 4 greater when $\gamma = 0.5$.

FIG. 7. A summary of the values of F_1, the nondimensional potential vorticity flux in the lower layer, obtained in the numerical integrations of the nonlinear model: (a) as a function of γ and α, with $\kappa = 0.1$; (b) as a function of κ and α, with $\gamma = 1.0$; and (c) as a function of γ and κ, with $\alpha = 0$. Contours are subjectively drawn.

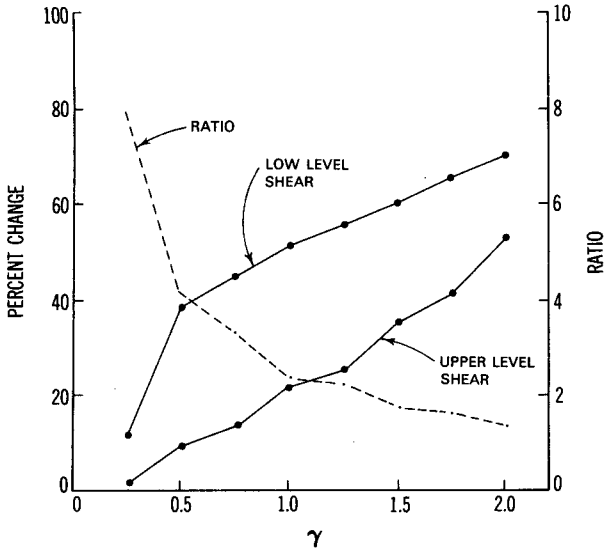

FIG. 8. Percent change in the dimensional lower-layer potential vorticity flux for a 10% change in the dimensional shear between the upper two layers and the lower two layers, as a function of γ, with $\kappa = 0.1$. The ratio (sensitivity to upper shear)/(sensitivity to lower shear) is also shown by the dashed line.

9. Concluding remarks

The eddy potential vorticity (PV) flux is the central quantity that one needs to understand if one hopes to formulate an eddy flux closure theory. The three-layer homogeneous turbulence model provides a relatively simple setting for studying the vertical structure of the PV flux and the relative importance of upper- and lower-tropospheric temperature gradients for the magnitude of the flux. In studying this model, we find that 1) the vertical structure of the most unstable mode on the time-mean flow provides a useful approximation to the vertical structure of the turbulent PV flux; 2) a "baroclinic adjustment" construction that allows one to estimate when the PV flux will be confined to the lowest two layers, and the extent to which it penetrates into the upper layer, also provides a fairly reliable prediction, although it underestimates the vertical penetration of the eddies when the vertical shear is small; and 3) in an atmospheric parameter setting (with negative PV gradient in the lower layer only) the lower-layer temperature gradient has a stronger influence on the magnitude of the PV fluxes than does the upper-layer gradient. For the same mean shear, curvature that concentrates the shear at low levels (where the mean PV gradient changes sign) gives rise to stronger eddies than curvature that concentrates the shear at upper levels, even though the eddies are deeper in the latter case.

The relevance of these results for more realistic *inhomogeneous* turbulent flows remains to be determined. Our intuition is that these results should remain qualitatively relevant for the *horizontally averaged* PV fluxes, or equivalently, the horizontally averaged heat fluxes, in inhomogeneous flows. However, they tell us little about the climatological momentum fluxes whose existence is a direct consequence of the horizontal inhomogeneity. A variety of results, particularly eddy life-cycle studies on the sphere (Simmons and Hoskins 1978), suggests that linear modal structures are of limited value in understanding momentum fluxes in the atmosphere, as these are tied to the final stages of barotropic decay in the upper troposphere. The momentum flux could be more sensitive than the heat flux to upper-level temperature gradients.

Acknowledgments. One of the authors (EOB) was supported while at GFDL by NOAA Grant NA87EA-D-OA039.

REFERENCES

Charney, J., 1971: Geostrophic turbulence. *J. Atmos. Sci.*, **28,** 1087–1095.

Davey, M. K., 1977: Baroclinic instability in a fluid with three layers. *J. Atmos. Sci.*, **34,** 1224–1234.

Green, J. S. A., 1970: Transfer properties of the large-scale eddies and the general circulation of the atmosphere. *Quart. J. Roy. Meteor. Soc.*, **96,** 157–185.

Haidvogel, D. B., and I. M. Held, 1980: Homogeneous quasi-geostrophic turbulence driven by a uniform temperature gradient. *J. Atmos. Sci.*, **37,** 2644–2660.

Held, I. M., 1978: The vertical scale of an unstable baroclinic wave and its importance for eddy flux parameterization. *J. Atmos. Sci.*, **35,** 414–432.

Hua, B.-L., and D. B. Haidvogel, 1986: Numerical simulations of the vertical structure of quasi-geostrophic turbulence. *J. Atmos. Sci.*, **43,** 2923–2936.

James, I., 1987: Suppression of baroclinic instability in horizontally sheared flow. *J. Atmos. Sci.*, **44,** 3710–3720.

Lindzen, R. S., and B. Farrell, 1980: The role of the polar regions in global climate, and a new parameterization of global heat transport. *Mon. Wea. Rev.*, **108,** 2064–2079.

Manabe, S., and R. Wetherald, 1975: The effect of doubling the CO_2 concentration on the climate of a general circulation model. *J. Atmos. Sci.*, **32,** 3–15.

Panetta, R. L., and I. M. Held, 1988: Baroclinic eddy fluxes in a one-dimensional model of quasi-geostrophic turbulence. *J. Atmos. Sci.*, **45,** 3354–3365.

Pedlosky, J., 1987: *Geophysical Fluid Dynamics.* 2d ed. Springer-Verlag, 710pp.

Rhines, P. B., 1975: Waves and turbulence on a β-plane. *J. Fluid Mech.*, **69,** 417–443.

Salmon, R. S., 1980: Baroclinic instability and geostrophic turbulence. *Geophys. Astrophys. Fluid Dyn.*, **15,** 167–211.

Satyamurty, P., V. B. Rao, and A. D. Moura, 1982: Subsynoptic scale baroclinic instability. *J. Atmos. Sci.*, **39,** 1052–1061.

Simmons, A. J., and B. J. Hoskins, 1978: The life cycles of some nonlinear baroclinic waves. *J. Atmos. Sci.*, **35,** 414–432.

Staley, D. O., 1986: Baroclinic and barotropic instability spectra as functions of N in N-level models. *J. Atmos. Sci.*, **43,** 1817–1832.

Stone, P. H., 1972: A simplified radiative-dynamical model for the static stability of rotating atmospheres. *J. Atmos. Sci.*, **29,** 405–418.

Stouffer, R. J., S. Manabe, and K. Bryan, 1989: Interhemispheric asymmetry in climate response to a gradual increase in atmospheric CO_2. *Nature,* **342,** 660–662.

Vallis, G. K., 1988: Numerical studies of eddy transport properties in eddy-resolving and parameterized models. *Quart. J. Roy. Meteor. Soc.*, **114,** 183–204.